Journal of Power Sources 196 (2011) 279–286

Contents lists available at ScienceDirect

Journal of Power Sources

journal homepage: www.elsevier.com/locate/jpowsour

Hydrogen release by thermolysis of ammonia borane NH_3BH_3 and then hydrolysis of its by-product [BNH_x]

U.B. Demirci*, S. Bernard, R. Chiriac, F. Toche, P. Miele

Université Lyon 1, CNRS, UMR 5615, Laboratoire des Multimatériaux et Interfaces, 43 boulevard du 11 Novembre 1918, F-69622 Villeurbanne, France

ARTICLE INFO

Article history:
Received 17 March 2010
Received in revised form 10 June 2010
Accepted 11 June 2010
Available online 20 June 2010

Keywords:
Ammonia borane
Hydrogen
Hydrolysis
Polyaminoborane
Solid-state hydrogen storage
Thermolysis

ABSTRACT

Ammonia borane (AB) is one of the most attractive hydrides owing to its high hydrogen density (19.5 wt%). Stored hydrogen can be released by thermolysis or catalyzed hydrolysis, both routes having advantages and issues. The present study has envisaged for the first time the combination of thermolysis and hydrolysis, AB being first thermolyzed and then the solid by-product believed to be polyaminoborane $[NH_2BH_2]_n$ (PAB) being hydrolyzed. Herein we report that: (i) the combination is feasible, (ii) PAB hydrolyzes in the presence of a metal catalyst (Ru) at 40 °C, (iii) a total of 3 equiv. H_2 is released from AB and PAB–H_2O, (iv) high hydrogen generation rates can be obtained through hydrolysis, and (v) the by-products stemming from the PAB hydrolysis are ammonium borates. The following reactions may be proposed: AB → PAB + H_2 and PAB + xH_2O → $2H_2$ + ammonium borates. All of these aspects as well as the advantages and issues of the combination of AB thermolysis and PAB hydrolysis are discussed.

1. Introduction

Solid-state storage is one of the main routes investigated to address the hydrogen storage issue and therein ammonia borane NH_3BH_3 (AB) is one of the most promising complex materials owing to its high hydrogen density (19.5 wt%) [1–3]. Recovering all of the stored hydrogen is, however, problematic and addressing such an issue is today the main challenge. For example, for automotive applications, it is expected that a gravimetric hydrogen storage capacity (GHSC) of 5.5 wt% is needed by 2015, with H_2 having to evolve at <85 °C [4]. It is important to note that this criterion considers the storage system as a whole (including the tank, storage media, safety system, valves, regulators, piping, mounting brackets, insulation, added cooling capacity, and any other balance-of-plant component) [4,5]. Assuming that the storage system components weight 50% of the total mass, the maximum effective gravimetric hydrogen density (GHD) of AB can only be 9.75 wt%.[1] In other words, AB must release 2 equiv. H_2 at 85 °C to be technologically viable. It is noteworthy that another great challenge with AB is off-board recyclability [2] because AB is not useable for reversible on-board hydrogen storage [6,7].

Dehydrogenation of AB can be done through two routes [1,8] that are thermolysis and hydrolysis. Thermolysis is a simple but harsh process. Hydrolysis is also a simple process but it is much less harsh than thermolysis. AB is stable in aqueous solution under inert atmosphere whereas it slowly hydrolyzes in air, which is associated with the catalytic effect of carbonic acid H_2CO_3 formed by dissolution of CO_2 in water [9]. Actually, hydrolysis has to be acid- [9] or metal-catalyzed [10]. Alcoholysis of AB has also been reported [11].

Thermolysis of AB can be described as a sequence of four processes occurring at high temperatures (104, 105–120, 120–200, 200–500 °C) [12,13]:

$$n\mathrm{NH_3BH_3(s)} \rightarrow n\mathrm{NH_3BH_3(l)} \quad (1a)$$

$$n\mathrm{NH_3BH_3(l)} \rightarrow [\mathrm{NH_2BH_2}]_n\mathrm{(s)} + n\mathrm{H_2(g)} \quad (1b)$$

$$[\mathrm{NH_2BH_2}]_n\mathrm{(s)} \rightarrow [\mathrm{NHBH}]_n\mathrm{(s)} + n\mathrm{H_2(g)} \quad (1c)$$

$$[\mathrm{NHBH}]_n\mathrm{(s)} \rightarrow [\mathrm{NB}]_n\mathrm{(s)} + n\mathrm{H_2(g)} \quad (1d)$$

After the AB melting (Eq. (1a)), polyaminoborane (PAB) and then polyiminoborane (PIB) form while 1 equiv. H_2 (i.e. GHD of 6.5 wt%) evolves at each stage (Eqs. (1b) and (1c), respectively). In other words, 2 equiv. H_2 are released at 100–200 °C, which implies a GHD of 13.0 wt% and so a GHSC of 6.5 wt%. But this is achieved at too high

* Corresponding author. Tel.: +33 04 72 44 84 03; fax: +33 04 72 44 06 18.
E-mail addresses: Umit.Demirci@univ-lyon1.fr, umitbilgedemirci@yahoo.fr (U.B. Demirci).

[1] Gravimetric hydrogen storage capacity, denoted GHSC, defines the capacity of a storage system taken as a whole (hydride + tank + pipes + valves + all of the other components). Gravimetric hydrogen density, denoted GHD, defines the gravimetric hydrogen storage capacity of the storage medium only (i.e. either the chemical hydride or the system hydride-water). It is noteworthy that the 2015 GHSC target for light-duty vehicular applications is 5.5 wt%. It can therefore be assumed a GHD of about 11 wt%.

0378-7753/$ – see front matter © 2010 Elsevier B.V. All rights reserved.
doi:10.1016/j.jpowsour.2010.06.031

temperatures, and thus one has to find a solution to decompose *n*AB into PIB and $2nH_2$ at <85 °C. To date, several solutions have been considered and showed promising results: namely, thermolysis in ionic liquid [14] or in organic solvent [15], insertion of AB into a scaffold material [16], transition metal complex catalysis [17] and solid-state catalysis [18]. For example, Denney et al. [17] observed a release of 1 equiv. H_2 within 14 min at room temperature for AB catalyzed by an Ir catalyst (0.5 mol% in tetrahydrofuran). And this result is a great step forward.

Catalyzed hydrolysis of AB ideally occurs in the presence of two water molecules at low temperatures (5–85 °C) [19]:

$$NH_3BH_3(aq) + 2H_2O(l) \rightarrow NH_4^+(aq) + BO_2^-(aq) + 3H_2(g) \quad (2)$$

The theoretical GHD of the system NH_3BH_3–H_2O is 15.0 wt%. Unfortunately NH_4^+ forms, which implies that 4H (3 per NH_3 and 1 per $2H_2O$) cannot be recovered. Accordingly, the theoretical GHD of NH_3BH_3–H_2O is lowered to 9.0 wt%. Recently, an effective GHD of 7.8 wt% (or a GHSC of 3.9 wt%) has been reported [20]. However that may be, such densities fall short of the 11 wt% (or 5.5 wt%) target. Nowadays, research on AB hydrolysis is emerging. For the time being, the studies have mainly focused on the development of active, durable catalytic materials [21–23].

Combination of thermolysis and hydrolysis has not been considered to date. The idea is as follows. While AB is being thermolyzed and H_2 is evolving, solid by-products, i.e. oligomers/polymers showing the structural unit [BNH_x], form [24]. Generally the dehydrogenation process is stopped at that moment. Alternatively, it could be envisaged to hydrolyze the solid by-products (denoted PAB as polyaminoborane for convenience). We have carried out such a study; AB was thermally decomposed to release about 1 equiv. H_2 and then the as-formed PAB was recovered to be hydrolyzed in the presence of a catalyst at low temperature. It is demonstrated for the first time that the combination of thermolysis and hydrolysis is feasible.

2. Experimental

2.1. Materials

Ammonia borane (AB, NH_3BH_3, Sigma–Aldrich, 97%), ruthenium chloride ($RuCl_3$, Strem Chemicals), cobalt chloride ($CoCl_2$, Acros Organics) and hexachloroplatinic acid (H_2PtCl_6, Sigma–Aldrich) were used as received and were handled in an argon-filled glove box. Deionized water was Millipore milli-q water with a resistivity >18 MΩ cm. In some cases, AB was doped with a metal chloride (10 wt% of metal). Typically, 450 mg of AB and 50 mg of metal were mechanically mixed together in a mortar and then ground, this being only done half an hour before the thermolysis experiment. In doing so, reproducible results were obtained in terms of thermal and calorimetric characterizations.

2.2. TGA and DSC

Thermogravimetric analyses (TGA) and differential scanning calorimetry (DSC) measurements were performed with TGA/SDTA 851^e and DSC1 (Mettler Toledo) under the following conditions: sample mass 2–3 mg, aluminum crucible of 100 μl with a pinhole, heating rate of 1 °C min^{-1}, and atmosphere of N_2 (50 ml min^{-1}). Both instruments were calibrated in the studied range of temperature, i.e. 25–220 °C min^{-1}. The melting points and melting enthalpies of four standards (gallium, naphthalene, indium and tin) were used for the calibration of the DSC in terms of heat flow, temperature and tau lag. Concerning the TGA, the melting points of five compounds (phenyl salycilate, naphthalene, benzoic acid, indium and tin) obtained from the DTA signals were used for the sample temperature calibration. Calcium oxalate was used for the sample mass calibration. It was found that in our experimental conditions (2–3 mg of sample, 1 °C min^{-1}) the error on the mass loss was 3.5% of the theoretical loss on the range 25–200 °C. As AB undergoes a voluminous swelling under heating, which may cause an artifact on the TGA profile or a contact with the internal wall of the TGA furnace [13], the AB mass was limited to 2–3 mg.

2.3. Thermal treatment

Neat AB and doped AB samples were thermally-treated at various temperatures, i.e. 100, 110 and 120 °C. AB was handled inside a N_2-filled glove box connected to the used furnace (Nabertherm). AB was transferred in a BN crucible, which was then transferred in the furnace. The furnace was subsequently pumped and refilled with N_2 before heating. A cycle of ramping at 1 °C min^{-1} was fixed to thermally-treat samples at the desired temperature 100, 110 or 120 °C in a N_2 flow (purity of 99.995%, 200 ml min^{-1}). Once the target temperature reached, the sample was cooled and transferred back in the glove box where it was ground and stored. The thermally-treated samples are denoted PAB_T with PAB as polyaminoborane and *T* as the temperature of the thermal treatment. The doped samples are denoted M-AB or M-PAB_T, with M as metal.

2.4. Hydrolysis

Hydrolysis was carried out as follows. In the glove box, the sample (90 ± 1 mg of neat AB or PAB_T, or 100 ± 1 mg of 10 wt% M-AB or 10 wt% M-PAB_T) was transferred into a glass tube (16 mm diameter), which was hermetically sealed with a silicon septum. The tube was then placed in a water bath at 40 ± 1 °C. The tube exhaust was connected to a water-filled inverted burette (water colored in blue). A cold trap maintained at a temperature lower than −140 °C was placed between the tube and the inverted burette, its role being to trap water vapor and any released ammonia. No stirring was used for the kinetic experiments, except the stirring action of the evolved hydrogen. Room temperature was 20 ± 1 °C. A volume of 2 ml of argon-purged distilled water (in the case of doped samples) or 2 ml of an aqueous (argon-purged distilled water) solution of metal chloride was injected into the tube (using a titration apparatus). The metal content was fixed at 10 wt% in any catalyzed reaction. Hydrogen evolved and displaced the liquid in the inverted burette. The experiments were video-recorded by using a camera connected to a computer. Time was controlled using the computer chronometer and a chronometer put near the burette (time evolution was also video-recorded). Hydrogen evolution was then analyzed using the software Matlab. Average hydrogen generation rate (HGR, ml(H_2) min^{-1} or l(H_2) min^{-1} g$^{-1}_{metal}$) and total conversion (TC, %) were calculated. HGR was calculated over a conversion range 10–50%, which does not take into account any induction period. TC was calculated as the ratio between the volume of H_2 generated and the maximum volume of H_2 generable. The measurements were repeated as least two times in order to ensure the results reproducibility. The purity of H_2 evolved was analyzed by both micro-chromatograph (μGC M200 from Agilent M Series; coupled to a mass selective detector) and Dräger tubes. We found that NH_3 evolved from PAB_T and its volume was <0.2 vol% of the gas stream in our experimental conditions (mol ratio H_2/NH_3 >500). As a result, its amount may be neglected in the calculations proposed hereafter. Nevertheless, a study about the undesired, detrimental NH_3 evolution is in progress.

2.5. Characterizations

AB, M-AB, PAB_T, M-PAB_T, their solid by-products and Ru after thermolysis/hydrolysis were analyzed by X-ray diffrac-

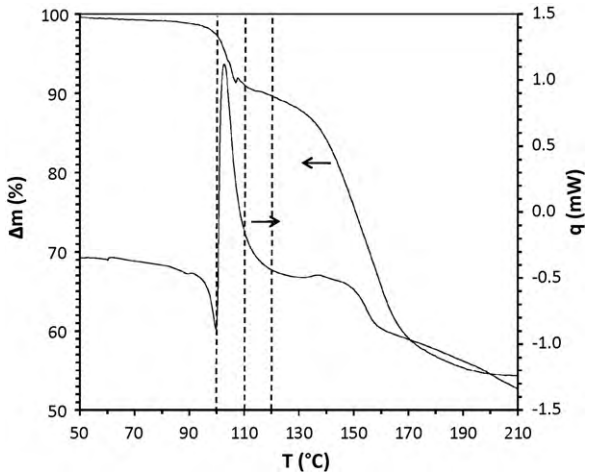

Fig. 1. Neat AB thermolysis: TGA (Δm (%) as a function of T (°C)) and DSC (q (mW) as a function of T (°C)) profiles.

tion (XRD, Bruker D5005 powder diffractometer, CuKα radiation (λ = 1.5406 Å)) and diffuse reflectance Fourier transform infrared spectroscopy (IR, FTIR Nicolet 380). Upon the hydrolysis completion, the by-products in aqueous solution were recovered, dried at 80 °C for 48 h and ground to be analyzed by XRD and IR. To isolate Ru, the slurry was handled according to the following cycle: washing, ultrasonication for 30 min, filtration (five times). The Ru catalyst was then dried at 80 °C overnight. By IR analysis, no trace of water or other insoluble compound was found (S.I. #1 (See Supplementary Information)). The Ru particle-free slurry and the washing solutions were analyzed by ICP-AES 'Activa' (wavelength 240.27, 245.55, 267.888 nm; at IRCELYON, UMR5256, University Lyon 1, CNRS, Lyon, France; by Yvon Jobin). It was found that <0.05 mol% of the used Ru were in the slurry. One may therefore assert than all Ru^{3+} cations had reduced.

3. Results and discussion

The primary objective of the present study was to assess the feasibility of the combination of AB thermolysis and PAB hydrolysis. It is noteworthy that decreasing the onset temperature of AB dehydrogenation was not really taken into consideration. Actually, it was beyond the scope of our study but it is an issue that will be addressed in a follow-up work.

3.1. Thermolysis of AB to obtain PAB

Neat AB was studied first. It was decomposed by thermolysis and then the stability of the PAB_T in water was assessed. The thermal decomposition of neat AB was followed by TGA and DSC (Fig. 1 and Table 1). It is characterized by two mass losses of 7.2 ± 0.2 and 35.0 ± 1.2 wt%, respectively (i.e. 1.11 ± 0.03 and 5.39 ± 0.18 equiv. H_2 assuming pure H_2 released). A mass loss higher than 6.5 wt% (1 equiv. H_2) is ascribed to the formation of undesired gaseous side-products such as borazine ($B_3N_3H_6$) or diborane (B_2H_6) [13]. In our experimental conditions, only $B_3N_3H_6$ as gaseous side-product was detected. No NH_3 was found. The DSC curve shows two exothermic processes and an endothermic peak (AB melting [25]) starting at 97 °C that partially compensates the first exothermic peak. In the present work, the TGA and DSC profiles had a notable interest in determining the temperature of the thermal treatments and thus three temperatures were chosen: 120 °C, the end of the first decomposition; 110 °C, in the course of the first decomposition; 100 °C, at the beginning of the first decomposition. At 120 °C, about 1 equiv. H_2 was released from AB; the as-formed PAB_{120} could then be used to be hydrolyzed. With respect to PAB_{100} and PAB_{110}, our objective was to analyze two of the intermediates formed during the decomposition of AB.

Table 1
Data from the TGA and DSC (heating rate 1 °C min^{-1}, $T \leq 120$ °C).

Sample	Onset T (°C)	Mass loss (%)	Equiv. H_2	NH_3 evolution
AB	99	7.2 ± 0.2	1.1	None
$RuCl_3$-doped AB[a]	100	7.9 ± 0.2	1.2	None

[a] The mass loss is that of AB only, the $RuCl_3$ weight being subtracted.

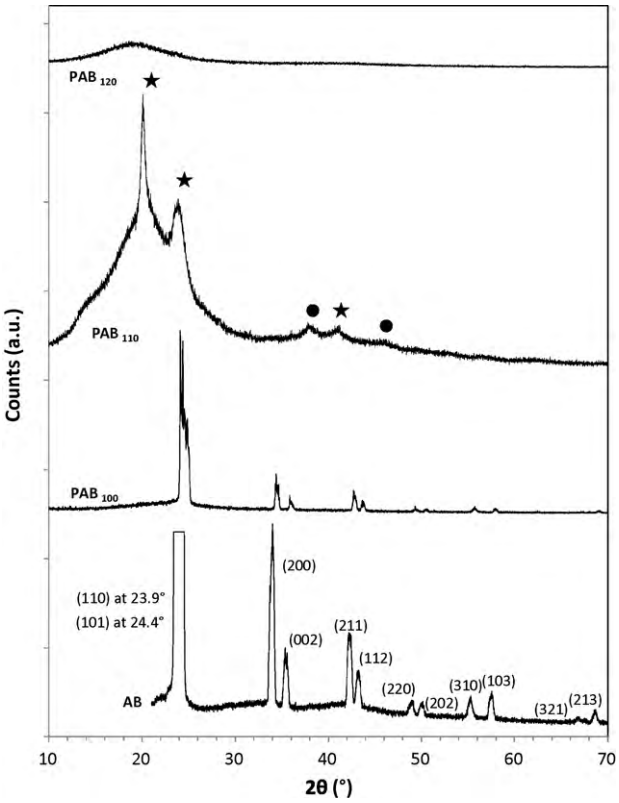

Fig. 2. XRD patterns of AB (for clarity, the intensity of the peak at about 24° has been cut), PAB_{100}, PAB_{110} (stars: $(BH_2NH_2)_5$ ICDD 00-019-0418; circles: $NH_3B_3H_7$ ICDD 01-076-0099), and PAB_{120}.

Neat AB, PAB_{100}, PAB_{110} and PAB_{120} were characterized by XRD. The XRD patterns (Fig. 2) clearly show the decomposition of AB. Indeed, a broad peak centered at $2\theta = 19.4°$, which is characteristic of the formation of amorphous $[NH_2BH_2]_n$ [12], is seen, mainly for PAB_{120}. At 100 °C, some AB is still observed, indicating that the thermolysis and the subsequent polymerization had initiated. Maybe diammoniate of diborane $[(NH_3)_2BH_2]^+[BH_4]^-$, which is an AB isomer yielded during the induction period of AB decomposition [26], formed. At 110 °C, a broad peak centered at around $2\theta = 19$–$20°$ and a sharper peak at $2\theta = 20.2°$ are depicted. They do not match reference patterns and makes the intermediate identification difficult. The former peak points to the formation of amorphous $[NH_2BH_2]_n$ whereas the latter one may be assigned to a borane amide $[BH_2NH_2]_5$ (ICDD 00-019-0418; $2\theta = 20.1°$, 23.6° and 41.1°). However, the peaks at $2\theta = 37.9°$ and 46.3° have not been found in the pattern of $[BH_2NH_2]_5$ but might be assigned to $NH_3B_3H_7$ (ICDD 01-076-0099). As a result, one may suggest that the XRD pattern of PAB_{110} shows the formation of oligomers and an amorphous polymer.

Neat AB, PAB_{100}, PAB_{110} and PAB_{120} were characterized by IR (Fig. 3). The bands were assigned using Refs. [24,27–30]. The spectra

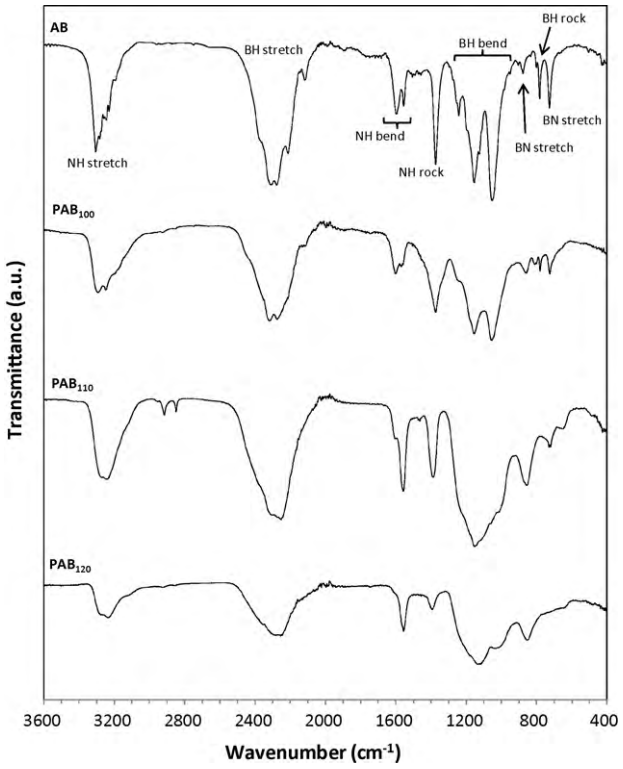

Fig. 3. IR spectra of AB, PAB_{100}, PAB_{110} and PAB_{120}.

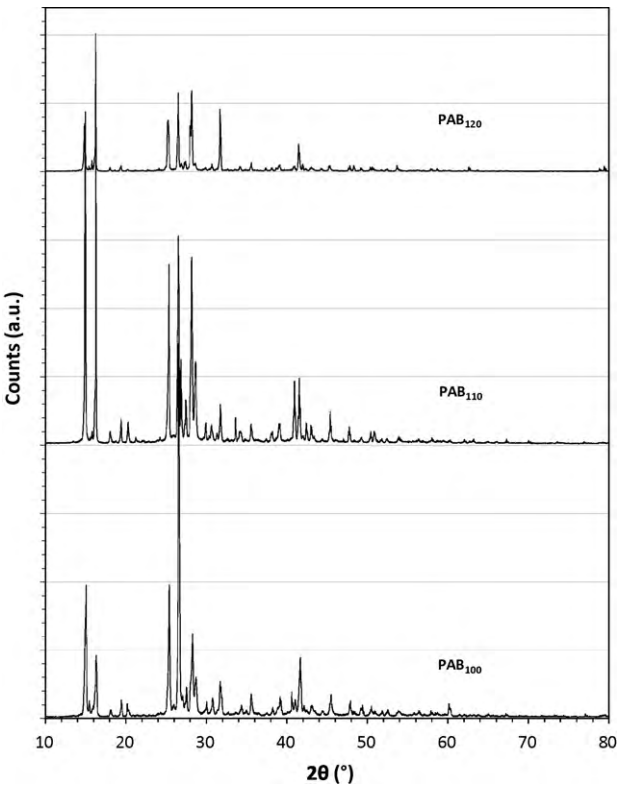

Fig. 4. XRD patterns of by-products recovered for hydrolysis (without catalyst) of PAB_{100}, PAB_{110} and PAB_{120}.

of both AB and PAB_{120} (i.e. $[NH_2BH_2]_n$) have been confirmed. The spectrum of PAB_{100} is quite similar to that of AB but few bands are broadened (e.g. NH rocking at 1367 cm^{-1}, BH bending at 1039 and 1141 cm^{-1}). PAB_{100} appears to be mainly composed of AB. PAB_{110} shows a spectrum similar to that of PAB_{120}.

PAB_{100}, PAB_{110} and PAB_{120} were hydrolyzed (without catalyst) at 40 °C. Few bubbles were observed. However, the HGR was very slow. The hydrolysis was then accelerated by increasing the temperature up to 80 °C without measuring the HGR. Upon the reaction completion, the by-products were dried for 48 h at 80 °C, ground and analyzed by both XRD and IR. The XRD patterns (Fig. 4) suggest the formation of a mixture of two ammonium borate hydrates: i.e. $NH_4B_5O_8{\cdot}3H_2O$ (ICDD 00-012-0637) and $NH_4B_5O_8{\cdot}4H_2O$ (ICDD 00-031-0043). It is difficult to state that one compound predominates over the other because all peaks cannot be assigned to a single compound and the borates share several peaks. Besides, a few broad peaks at around $2\theta = 28°$, 35° and 42° slightly deviate the background, which is characteristic of the existence of amorphous borates [31] as well as that of very small crystallites. This strongly suggests that the by-product composition is much more complex than that reported heretofore, amorphous borates very likely forming in our experimental conditions. On the other hand, the XRD patterns suggest the evolution of NH_3. Even though no NH_3 was found in the gas stream evolving from AB thermal decomposition, NH_3 was slightly smelt in the hydrolysis tube but much in the oven atmosphere in the course of the drying stage at 80 °C. Actually such a situation is problematic since it means that some NH_3 can evolve, which is detrimental to fuel cell application [32]. A deeper study about NH_3 evolution from AB is especially in progress but this aspect is not discussed hereafter, being beyond the scope of the primary objective of the present investigation. Be that as it may, the main thing that stands out is that $[NH_2BH_2]_n$ hydrolyzes into borates.

The IR spectra of the PAB_T by-products are similar. Accordingly, only the IR spectrum of the PAB_{120} by-products is shown in Fig. 5 (the others are given in S.I. #2). The bands were assigned using Refs. [33–35] and the IR spectra support the formation of ammonium borate hydrates.

As a summary of the present sub-section, the following reactions, i.e. thermolysis of AB and hydrolysis of PAB_{120}, may be proposed (only one by-product, namely $NH_4B_5O_8{\cdot}4H_2O$, is taken into account):

$$n NH_3BH_3 \rightarrow [NH_2BH_2]_n + n H_2@120\,^{\circ}C \quad (3a)$$

$$[NH_2BH_2]_n + 12n/5 H_2O \rightarrow n/5 NH_4B_5O_8{\cdot}4H_2O + 4n/5 NH_3 + 2n H_2@80\,^{\circ}C \quad (3b)$$

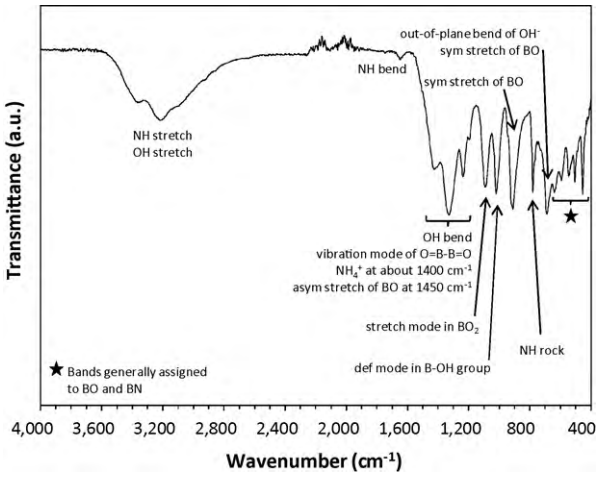

Fig. 5. IR spectrum of the by-products recovered after the hydrolysis (without catalyst) of PAB_{120}.

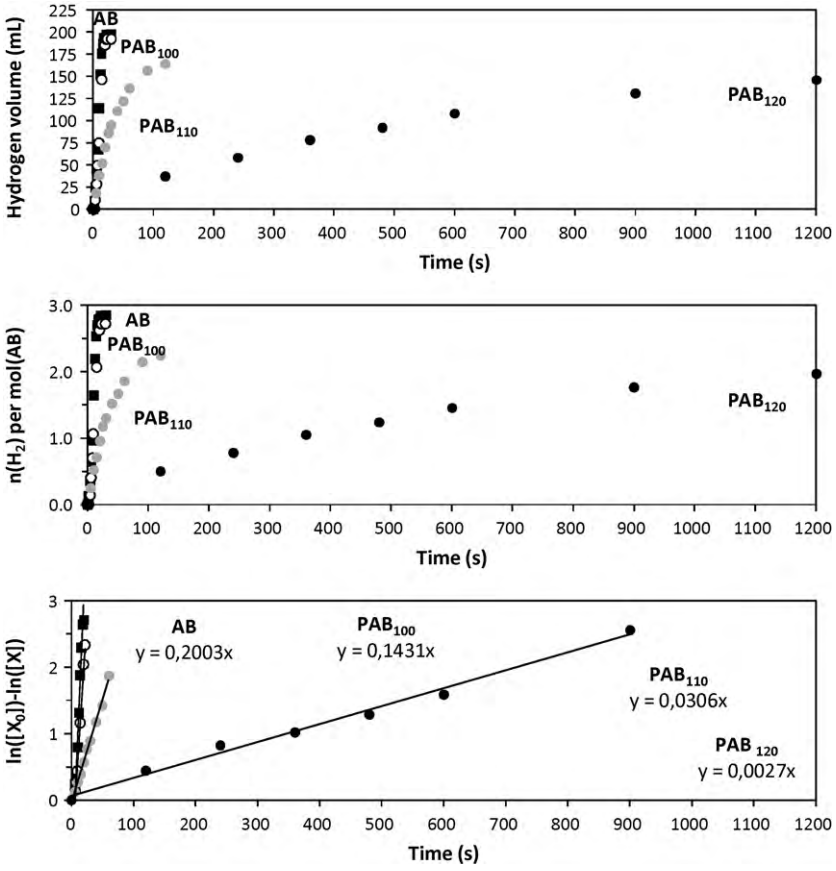

Fig. 6. Hydrogen evolutions for $RuCl_3$-catalyzed hydrolysis of AB, PAB_{100}, PAB_{110} and PAB_{120} at 40 °C; the top figure shows the evolution of V(H_2, ml) with time; the middle figure shows the evolution of $n(H_2)$ per mol(AB) with time; the bottom figure shows the variation of $\ln[AB]_0 - \ln[AB]_t$ with time.

The resulting GHD and GHSC are 8.1 and 4.05 wt% if only the stoichiometric amount of water is considered.

3.2. Catalyzed hydrolysis of AB and PAB

AB, PAB_{100}, PAB_{110} and PAB_{120} were hydrolyzed in the presence of a catalyst. $RuCl_3$ was chosen as the catalyst precursor because (i) Ru is among the most active metals in the hydrolysis of boron hydrides and amine-borane adducts [36,37], (ii) metal chlorides are efficient in solvolyzing boron hydrides and amine-borane adducts [11,38], and (iii) $RuCl_3$ reduces into stable Ru^0 [39] (for some transition metals such as Co the active specie is not stable, being a compound consisting of Co and B, and it is unclear whether it is a boride or an alloy [38,40,41]). Fig. 6 shows the hydrogen evolutions. The following observations stand out:

- In the presence of Ru, AB hydrolyzes and ~200 ml(H_2), i.e. 2.90 ± 0.05 mol(H_2) per mol(AB), evolves. This is in accordance with Eq. (2) [10,19].
- The Ru-catalyzed hydrolysis of PAB_{100} generates ~190 ml(H_2), i.e. 2.7 ± 0.05 mol(H_2) per mol(AB). The formula $NH_{2.7}BH_{2.7}$ may be suggested. PAB_{100} is none other than liquid AB that has solidified when the sample was cooled. Hence it is likely that PAB_{100} mainly consists of AB and/or diammoniate of diborane $[(NH_3)_2BH_2]^+[BH_4]^-$ [26].
- For AB and PAB_{100}, the HGRs are 684 and 624 ml(H_2) min^{-1}, respectively, or 68.4 and 62.4 l(H_2) min^{-1} g^{-1}_{Ru}. Despite discrepancies in the experimental conditions and H_2 release systems, they favorably compare rates reported up to now [42].
- With respect to PAB_{110}, ~165 ml(H_2) was released. The volume of H_2 is lower than that recorded for both AB and PAB_{100}. Assuming

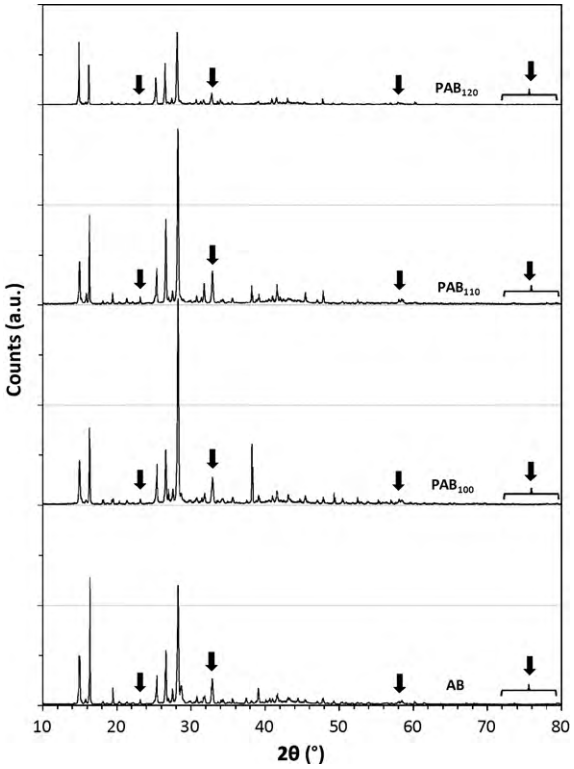

Fig. 7. XRD patterns of the by-products recovered for Ru-catalyzed hydrolysis of AB, PAB_{100}, PAB_{110} and PAB_{120}; the black arrows indicate the peaks attributed to NH_4Cl (ICDD 01-077-2352).

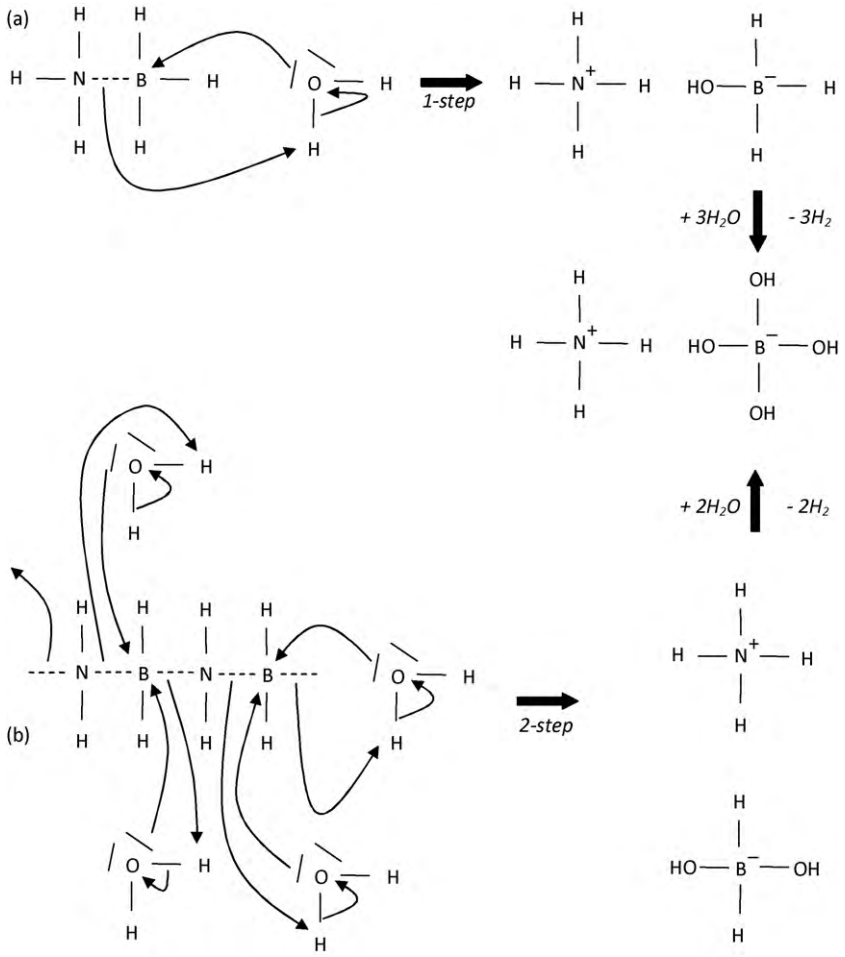

Fig. 8. Illustration of the hydrolysis of (a) AB and (b) PAB: simplified reaction mechanisms.

PAB_{110} is $[NH_2BH_2]_n$, 150 ml(H_2), i.e. 2 mol(H_2) per mol(NH_2BH_2), should have evolved but the H_2 evolution shows that the H content in PAB_{110} is higher than that in PAB_{120}. Accordingly the formula $NH_{2.2}BH_{2.2}$ may be ascribed to the monomer of PAB_{110}.

- PAB_{120} generated about 150 ml(H_2); 2.00 ± 0.05 mol(H_2) per mol(NH_2BH_2) evolved in >20 min. This confirms that the structural unit of PAB_{120} may be NH_2BH_2.

To summarize, it appears that AB ~ PAB_{100} > PAB_{110} > PAB_{120} in terms of both volume of H_2 evolved and HGR. The most significant result is that $[NH_2BH_2]_n$ is hydrolyzed at 40 °C in the presence of a catalyst. An equiv. of 3 mol(H_2) may be recovered from 1 mol(AB) by thermolysis at 120 °C and then by hydrolysis of PAB_{120} at 40 °C, 33% of H being provided by water. Fig. 6 also shows that the hydrolysis of AB, PAB_{100}, PAB_{110} and PAB_{120} are first-order processes and the resulting rate constants are 0.20, 0.14, 3.1×10^{-2} s^{-1} and 2.7×10^{-3} s^{-1}.

The solid by-products stemming from AB and PAB_T were recovered, dried, ground and analyzed by XRD and IR. The XRD patterns (Fig. 7) are rather similar. Compared to reference patterns, various ammonium borate hydrates have been identified: i.e. $NH_4B_5O_8 \cdot 3H_2O$ (ICDD 00-012-0637), $NH_4B_5O_8 \cdot 4H_2O$ (ICDD 00-031-0043) and $(NH_4)_2B_4O_7 \cdot 4H_2O$ (ICDD 00-019-0061). Further, ammonium chloride NH_4Cl (ICDD 01-077-2352) can be suggested (especially regarding the peaks at around $2\theta = 23.3°$, 32.9°, 58.0° and >70.0°). Like in Fig. 4, the formation of amorphous borates as well as small crystallites that are invisible or partly visible by XRD cannot be discarded. The IR spectra (S.I. #3) are similar to those of the by-products stemming from the uncatalyzed samples (Fig. 5), suggesting the formation of ammonium borate hydrates.

To summarize, it has been showed that $[NH_2BH_2]_n$ partially dehydrogenates at acceptable rates by hydrolysis in the presence of $RuCl_3$, resulting in the evolution of 2 equiv. H_2 and formation of ammonium borate hydrates, half of H_2 being provided by water. Thereby, 3 equiv. H_2 per AB can be liberated. Assuming the hydrolysis reaction is stoichiometric, the combination of thermolysis and hydrolysis should require $2H_2O$:

$$n NH_3BH_3 \rightarrow [NH_2BH_2]_n + n H_2 \quad (4a)$$

$$[NH_2BH_2]_n + 2n H_2O \rightarrow 2n H_2 + n NH_4BO_2 \quad (4b)$$

$$\text{Sum of 4a + 4b}: n NH_3BH_3 + 2n H_2O \rightarrow 3n H_2 + n NH_4BO_2 \quad (4c)$$

The resulting GHD and GHSC are 8.1 and 4.05 wt% (taking into account the catalyst weight). These values are the highest ones and decrease with the increasing amount of water as well as the hydratation of the hydrolysis by-products. In the present experimental conditions, the GHD and GHSC are 0.9 and 0.45 wt% (mol ratio H_2O/AB of 36). A simplified reaction mechanism accounting for the hydrolysis of PAB is proposed in Fig. 8.

3.3. Alternative approaches

The utilization of other catalyst precursors (i.e. $CoCl_2$ [43] and H_2PtCl_6 [38]) and mixing the catalyst precursor $RuCl_3$ together with

AB [20] were also considered. The latter approach envisaged the preparation of $RuCl_3$-loaded AB that was first thermolyzed and then hydrolyzed.

$CoCl_2$ and H_2PtCl_6 were tested in the hydrolysis of AB and PAB_{120} (S.I. #4). With respect to the AB hydrolysis, there are three observations. First, H_2 evolves more rapidly when AB is catalyzed by $RuCl_3$ (684 ml(H_2) min^{-1}) than it does when catalyzed by $CoCl_2$ (214 ml(H_2) min^{-1}) or H_2PtCl_6 (185 ml(H_2) min^{-1}). Second, consistently with Eq. (2), about 3 mol(H_2) per mol(AB) evolve. Third, there is an induction period of about 1 min for the $CoCl_2$-catalyzed hydrolysis; during this period, Co^{2+} is reduced by AB to form the active Co specie, i.e. a Co–B alloy or a cobalt boride (CoB, Co_2B or Co_3B) [38,40,41]. Regarding the PAB_{120} hydrolysis, both $CoCl_2$ and H_2PtCl_6 catalyze the reaction, ~150 ml(H_2) evolving in about 30 and 50 min. As a result, $RuCl_3 > CoCl_2 > H_2PtCl_6$ in terms of HGR (12, 6 and 5 ml(H_2) min^{-1}, respectively). In each reaction, total conversions of 100% were achieved. The by-products were analyzed by XRD and IR. The XRD patterns (S.I. #5) are quite complex. Various ammonium borate hydrates ($NH_4B_5O_8{\cdot}3H_2O$ ICDD 00-012-0637, $NH_4B_5O_8(H_2O)_4$ ICDD 01-074-1233 and 00-031-0043, $(NH_4)_2B_4O_7{\cdot}4H_2O$ ICDD 00-019-0061) and NH_4Cl (ICDD 01-077-2352) were found as being possible. Like the previous XRD-based observations, amorphous borates are likely to form. The IR spectra (S.I. #6) are similar to those presented heretofore and support the formation of borates.

The 2nd approach aimed at mixing $RuCl_3$ (10 wt%) and AB together. The thermal decomposition of Ru–AB was studied by TGA and DSC. Actually the presence of $RuCl_3$ in the matrix of AB had no effect on the onset temperature of the AB decomposition, the TGA and DSC profiles (S.I. #7) being similar to those obtained with neat AB (Fig. 1). Regardless of this inefficiency, the study went on. Ru–PAB_{120} was obtained by thermal treatment at 120 °C and was analyzed by XRD and IR. The XRD pattern (S.I. #8) shows two broad peaks centered at around $2\theta = 17°$ and 42° that are characteristic of amorphous $[NH_2BH_2]_n$. Furthermore it shows several other peaks. The XRD pattern does not match the reference patterns of $RuCl_3$ and Ru^0 but it matches that of ruthenium amine chloride $Ru(NH_3)_6Cl_2$ (ICDD 00-024-0991). The IR spectrum (S.I. #9) of Ru–PAB_{120} is quite similar to that of PAB_{120} (Fig. 3) but the band at 1387 cm^{-1} (BN stretching) is larger while overlapping that at 1518 cm^{-1} (NH stretching) and the band at 656 cm^{-1} (BN stretching) is stronger. The spectrum is also similar to that reported in Ref. [24] for $[NH_2BH_2]_n$. Ru–PAB_{120} was then hydrolyzed. At 40 °C, ~96 ml(H_2) evolved in 6 min. In other words, 1.3 equiv. H_2 evolved. Compared to PAB_{120} catalyzed by $RuCl_3$, Ru–PAB_{120} is much less efficient in terms of conversion (~64%) and HGR. The origin of this is not yet understood. The by-products were recovered and analyzed by XRD (S.I. #8) and IR (S.I. #9). They were found as being similar to those reported in the previous sections. The Ru nature was also considered after hydrolysis. The Ru-based black solid was separated from the by-products and analyzed by XRD (S.I. #10). Ru^0 has been identified, implying that Ru^{3+} had reduced.

To summarize the present sub-section, it has been showed that both of the alternative approaches discussed are achievable but they need further studies in order to improve their efficiency. It is especially true for the 2nd approach, which is in our opinion the most attractive.

4. Conclusion and prospects

PAB, i.e. $[NH_2BH_2]_n$, does hydrolyze at 40 °C with the aid of a Ru catalyst (i.e. $RuCl_3$). It is what has been showed heretofore. Our idea was as follows. First, AB was decomposed by thermolysis at 120 °C, 1 equiv. H_2 being evolved. The solid by-product that was recovered was $[NH_2BH_2]_n$ (PAB). Second, PAB was partly dehydrogenated through Ru-catalyzed hydrolysis at near-ambient conditions, 2 equiv. H_2 being evolved. The hydrolysis of PAB led to the formation of by-products suggested as being ammonium borate hydrates (nevertheless further studies are required to identify the amorphous by-products formed). Through such dehydrogenations, 3 equiv. H_2 evolved. Further, the H_2 release was measured to be fast.

Against AB proper thermolysis, the combination of AB thermolysis and PAB hydrolysis may be of interest owing to the following aspects. The 2nd equiv. H_2 is evolved at near-ambient conditions while the thermolysis of PAB requires temperatures >120 °C. The purity of the 2nd equiv. H_2 generated by hydrolysis of PAB should be better with no emission of $B_3N_3H_6$ or B_2H_6; nevertheless NH_3 evolves in the course of the PAB hydrolysis, and can be detrimental to fuel cell (technical target: selectivity of <0.1 ppm). HGRs higher than those reported for PAB thermolysis can be achieved. Recyclability of the borate by-products might be easier than that of $[NHBH]_n$ due to the fact it has already been suggested for borates stemming from hydrolysis of $NaBH_4$ [44]. In other words, such dehydrogenation reactions might be envisaged to dehydrogenate AB if an efficient way to decrease the onset temperature of Eq. (1c) is not found.

The combination of AB thermolysis and PAB hydrolysis is effective but it has to be improved, especially in terms of temperature of 1st dehydrogenation and GHD. $RuCl_3$ has showed to be inefficient in decreasing the onset temperature of 1st dehydrogenation of AB. From an application point of view, the temperature should be decreased to <85 °C and this could be achieved e.g. with the aid of more efficient catalytic material or doping agent [17]. Besides, such a catalyst must be reactive in catalyzing hydrolysis of PAB. Finding such a catalyst was beyond the scope of the present study, but this is obviously a critical issue. Regarding the GHD, using liquid water is in fact detrimental to the effective HD of the system PAB–H_2O. Assuming that only stoichiometric amounts of water (namely, 2 mol) are required, the highest theoretical GHD is 9.0 wt% (8.1 wt% in the presence of 10 wt% catalyst). It is lower than the claimed 13.0 wt% achieved by thermolysis of AB. To optimize the GHD, steam (H_2O (g)) from a fuel cell could be used [45]; as a result, GHDs and GHCSs up to 19.5 and 9.75 wt% could be reached, making then AB suitable for automotive applications in 2015 [4]. Compared to the direct hydrolysis of AB (Eq. (2)) with H_2O (g), the present approach has the advantage not to on-board store any H_2O (l), H_2O (l) being required to start hydrolysis before a fuel cell generates H_2O (g). Typically, AB thermolysis will generate H_2 that will be converted into H_2O (g) in the fuel cell, H_2O (g) being then recovered to hydrolyze PAB. Further, such an approach could help in heat management. Heat required to thermolyze AB could be recovered from the whole hydrogen storage-fuel cell system. It is evident that such an approach complicates the storage system but it brings solutions in avoiding on-board H_2O (l) storage, in heat management and in H_2/battery utilization.

To summarize, the combination of AB thermolysis and PAB hydrolysis is a new, alternative approach. It especially brings solutions to few of the issues faced with thermolysis of AB. Nevertheless, the approach has its own issues and further studies are now required to optimize the catalytic efficiency in thermolysis, the amount of H_2O in PAB hydrolysis and so the GHD/GHSC.

Acknowledgement

The present study was funded by ANR (project 'BoraHCx').

Appendix A. Supplementary data

Supplementary data associated with this article can be found, in the online version, at doi:10.1016/j.jpowsour.2010.06.031.

References

[1] P. Wang, X.D. Kang, Dalton Trans. (2008) 5400–5413.
[2] C.W. Hamilton, R.T. Baker, A. Staubitz, I. Manner, Chem. Soc. Rev. 38 (2009) 279–293.
[3] T. Umegaki, J.M. Yan, X.B. Zhang, H. Shioyama, N. Kuriyama, Q. Xu, Int. J. Hydrogen Energy 34 (2009) 2303–2310.
[4] U.S. Department of Energy, Office of Energy Efficiency and Renewable Energy and The FreedomCAR and Fuel Partnership, Targets for Onboard Hydrogen Storage Systems for Light-duty Vehicles, September 2009, available at http://www.eere.energy.gov.
[5] D. Mori, H. Hirose, Int. J. Hydrogen Energy 34 (2009) 4569–4574.
[6] U. Eberle, M. Felderhoff, F. Schüth, Angew. Chem. Int. Ed. 48 (2009) 2–25.
[7] T.K. Mandal, D.H. Gregory, Annu. Rep. Prog. Chem. Sect. A 105 (2009) 21–54.
[8] U.B. Demirci, P. Miele, Energy Environ. Sci. 2 (2009) 627–637.
[9] M. Chandra, Q. Xu, J. Power Sources 159 (2006) 855–860.
[10] M. Chandra, Q. Xu, J. Power Sources 156 (2006) 190–194.
[11] P.V. Ramachandran, P.D. Gagare, Inorg. Chem. 46 (2007) 7810–7817.
[12] M.G. Hu, R.A. Geanangel, W.W. Wendlandt, Thermochim. Acta 23 (1978) 249–255.
[13] V. Sit, R.A. Geanangel, W.W. Wendlandt, Thermochim. Acta 113 (1987) 379–382.
[14] M.E. Bluhm, M.G. Bradley, R. Butterick III, U. Kusari, L.G. Sneddon, J. Am. Chem. Soc. 128 (2006) 7748–7749.
[15] T. Wideman, S.G. Sneddon, Inorg. Chem. 34 (1995) 1002–1003.
[16] A. Gutowska, L. Li, Y. Shin, C.M. Wang, X.S. Li, J.C. Linehan, R.S. Smith, B.D. Kay, B. Schmid, W. Shaw, M. Gutowski, T. Autrey, Angew. Chem. Int. Ed. 44 (2005) 3578–3582.
[17] M.C. Denney, V. Pons, T.J. Hebden, D.M. Heinekey, K.I. Goldberg, J. Am. Chem. Soc. 128 (2006) 12048–12049.
[18] F. Cheng, H. Ma, Y. Li, J. Chen, Inorg. Chem. 46 (2007) 788–794.
[19] Q. Xu, M. Chandra, J. Power Sources 163 (2006) 364–370.
[20] U.B. Demirci, P. Miele, J. Power Sources 195 (2010) 4030–4035.
[21] T. Umegaki, J.M. Yan, X.B. Zhang, H. Shioyama, N. Kuriyama, Q. Xu, Int. J. Hydrogen Energy 34 (2009) 3816–3822.
[22] X. Yang, F. Cheng, J. Liang, Z. Tao, J. Chen, Int. J. Hydrogen Energy 34 (2009) 8785–8791.
[23] K.S. Eom, K.W. Cho, H.S. Kwon, Int. J. Hydrogen Energy 35 (2010) 181–186.
[24] J. Baumann, F. Baitalow, G. Wolf, Thermochim. Acta 430 (2005) 9–14.
[25] G. Wolf, J. Baumann, F. Baitalow, F.P. Hoffmann, Thermochim. Acta 343 (2000) 19–25.
[26] A.C. Stowe, W.S. Shaw, J.C. Linehan, B. Schmid, T. Autrey, Phys. Chem. Chem. Phys. 9 (2007) 1831–1836.
[27] J. Smith, K.S. Seshadri, D. White, J. Mol. Spectrosc. 45 (1973) 327–337.
[28] R. Komm, R.A. Geanangel, R. Liepins, Inorg. Chem. 22 (1983) 1684–1686.
[29] D.P. Kim, K.T. Moon, J.G. Kho, J. Economy, C. Gervais, F. Babonneau, Polym. Adv. Technol. 10 (1999) 702–712.
[30] B.H. Stuart, Infrared Spectroscopy: Fundamentals and Applications, John Wiley and Sons Ltd., 2004.
[31] Y. Kojima, Y. Kawai, H. Nakanishi, S. Matsumoto, J. Power Sources 135 (2004) 36–41.
[32] J. Yang, A. Sudik, C. Wolverton, D.J. Siegel, Chem. Soc. Rev. 39 (2010) 656–675.
[33] A. Kanturk, M. Sari, S. Piskin, Korean J. Chem. Eng. 25 (2008) 1331–1337.
[34] B. Molina Concha, M. Chatenet, C. Coutanceau, F. Hahn, Electrochem. Commun. 11 (2009) 223–226.
[35] N. Patel, R. Fernandes, G. Guella, A. Miotello, Appl. Catal. B 95 (2010) 137–143.
[36] U.B. Demirci, F. Garin, J. Alloys Compd. 463 (2008) 107–111.
[37] S. Basu, A. Brockman, P. Gagare, Y. Zheng, P.V. Ramachandran, W.N. Delgass, J.P. Gore, J. Power Sources 188 (2009) 238–243.
[38] H.I. Schlesinger, H.C. Brown, A.E. Finholt, J.R. Gilbreath, H.R. Hoekstra, E.K. Hyde, J. Am. Chem. Soc. 75 (1953) 215–219.
[39] F. Durap, M. Zahmakiran, S. Özkar, Int. J. Hydrogen Energy 34 (2009) 7223–7230.
[40] H.B. Dai, Y. Liang, L.P. Ma, H.M. Cheng, J. Phys. Chem. C 112 (2008) 15886–15892.
[41] B.H. Liu, Z.P. Li, L.L. Chen, J. Power Sources 180 (2008) 530–534.
[42] U.B. Demirci, O. Akdim, J. Andrieux, J. Hannauer, R. Chamoun, P. Miele, Fuel Cells 10 (2010) 335–350.
[43] O. Akdim, U.B. Demirci, D. Muller, P. Miele, Int. J. Hydrogen Energy 34 (2009) 2631–2637.
[44] Ç. Çakanyildirim, M. Gürü, Int. J. Hydrogen Energy 33 (2008) 4634–4639.
[45] E.Y. Marrero-Alfonso, J.R. Gray, T.A. Davis, M.A. Matthews, Int. J. Hydrogen Energy 32 (2007) 4117–4122.